

# Preparation and characterization of $\text{LiMn}_2\text{O}_4$ and $\text{LiCo}_{0.16}\text{Mn}_{1.84}\text{O}_4$ as cathode materials for lithium-ion batteries by low heating solid state coordination method

YUDAI HUANG, JUAN LI, DIANZENG JIA\*

*Institute of Applied Chemistry, Xinjiang University, Urumqi 830046, Xinjiang, People's Republic of China*

*E-mail: jdz@xju.edu.cn*

**Published online:** 15 May 2006

Spinel lithium manganese oxide  $\text{LiMn}_2\text{O}_4$  and its substituted forms  $\text{LiCo}_{0.16}\text{Mn}_{1.84}\text{O}_4$  were prepared by annealing of the mixed precursors which were synthesized by low heating solid state coordination method using lithium acetate, cobalt acetate, manganese acetate and oxalic acid as starting materials. The structures and morphologies of the  $\text{LiMn}_2\text{O}_4$  and  $\text{LiCo}_{0.16}\text{Mn}_{1.84}\text{O}_4$  were investigated as a function of annealing temperature. The results show that all samples in different annealing temperature have the same spinel structure. The higher the annealing temperature, the more complete the crystal structure, and the larger the particle size. In addition, the  $\text{LiMn}_2\text{O}_4$  and  $\text{LiCo}_{0.16}\text{Mn}_{1.84}\text{O}_4$  were used as cathode active materials for lithium secondary batteries and their charge/discharge properties have been investigated. As a result, it could be seen that low heating solid state coordination method is an effective method to prepare lithium manganese oxide ( $\text{LiMn}_2\text{O}_4$ ) and its substituted forms.

© 2006 Springer Science + Business Media, Inc.

## 1. Introduction

The technological advancement in the area of electronics and the onset of electric vehicles necessitate low cost, environment friendly and high energy density lithium-ion batteries. As a part of these requirements, lithium manganese oxide ( $\text{LiMn}_2\text{O}_4$ ) is considered to be more attractive cathode material for lithium-ion batteries than the competitors such as lithium cobalt or lithium nickel oxides, because of low cost, and acceptable environmental characteristics [1–5]. Unfortunately,  $\text{LiMn}_2\text{O}_4$  can exhibit significant capacity fading during charge/discharge cycle [6–8]. The reason for capacity fading is supposed to be linked to some possible factors, such as: (i) the fracture of structure due to repeated cycle; (ii) decomposition of the electrolyte at high-voltage region; (iii) the dissolution of  $\text{Mn}^{3+}$  ions into the electrolyte [1]. Many researchers have paid much attention on how to suppress the capacity loss of  $\text{LiMn}_2\text{O}_4$  during cycling [1, 7, 9]. It has been reported that the substituted manganese spinel compounds  $\text{LiM}_y\text{Mn}_{2-y}\text{O}_4$  ( $M = \text{Co}, \text{Ni}, \text{Cr}, \text{and Al}$ ) have

been prepared by solid state reaction and improved in cycle performance significantly comparing with that of parent  $\text{LiMn}_2\text{O}_4$  [10, 11]. The good cycle performance has been explained by the relatively stronger metal-oxygen bonding in the substituted spinel than that in  $\text{LiMn}_2\text{O}_4$  [10–12].

It should be noted that the lithium manganese oxide is usually made by solid state reactions, which involves the mechanical mixing of oxides and/or carbonates. These reactions usually require a long firing time and several grinding during the heating process, and moreover, it is difficult to control the particle size of the product. In recent years, there has been considerable interest in producing materials with various powder morphology, bulk density and stoichiometry by the liquid-phase reaction [13, 14]. It is well known that the sol-gel technique has been widely used for a homogeneous process. However, sol-gel method for preparing is also not an economical one because it involves long heating time and complex synthesis process to get the final powders.

\*Author to whom all correspondence should be addressed.

It has been confirmed that low heating solid state coordination method is a simple and effective method to fabricate a number of chemical compound. Cluster compounds, coordination compounds and solid-coordination compounds etc., have been synthesized by this method in the past years [15–17]. Especially, oxides and sulfides nanoparticles were firstly synthesized by our laboratory [18, 19]. In this work,  $\text{LiMn}_2\text{O}_4$  and its substituted forms spinel  $\text{LiCo}_{0.16}\text{Mn}_{1.84}\text{O}_4$  have been prepared by a simply annealing the mixed precursors which were synthesized by low heating solid state coordination method. The particle characteristics, such as crystallite size, microstructure and particle size etc., and electrochemical properties of these compounds have been also investigated.

## 2. Experimental

### 2.1. Sample preparation

$\text{LiMn}_2\text{O}_4$  and  $\text{LiCo}_{0.16}\text{Mn}_{1.84}\text{O}_4$  powders were prepared by using  $\text{LiAc} \cdot \text{H}_2\text{O}$ ,  $\text{Mn}(\text{Ac})_2 \cdot 4\text{H}_2\text{O}$ ,  $\text{Co}(\text{Ac})_2 \cdot 4\text{H}_2\text{O}$  and  $\text{H}_2\text{C}_2\text{O}_4 \cdot 2\text{H}_2\text{O}$  as starting materials. Metal acetate was measured with atomic ratio (Li: Mn = 1: 2 or Li: Co: Mn = 1: 0.16: 1.84) and mixed in an agate mortar. Before mixing, each of the starting materials was ground into powders, respectively. Grinding the mixture in an agate mortar with a pestle for 1.5 h in order to make it fully react and get the best possible homogeneity. Mixed precursor was obtained. Putting the mixed precursor into an oven at  $90^\circ\text{C}$  for 4 h to dry it.  $\text{LiMn}_2\text{O}_4$  and  $\text{LiCo}_{0.16}\text{Mn}_{1.84}\text{O}_4$  powders were obtained by annealing the precursor for 6 h at different temperatures in air in a muffle furnace, respectively, and then quenched to room temperature.

### 2.2. Characterization

The thermal decomposition behavior of the mixed precursor was examined by thermogravimetric analysis (TGA) and differential thermal analysis (DTA)(TGA-DTA, STA499, NETZSCH, Germany) at a heating rate of  $10^\circ\text{C}/\text{min}$ . Powder X-ray diffraction (XRD, MXP18AHF, MAC, Japan) using  $\text{CuK}\alpha$  radiation was used to identify the crystalline phase of the resulting materials. The grain size and morphology of the products were observed using an accelerating voltage of 100 kV transmission electron microscope (TEM, H-600, HITACHI, Japan).

### 2.3. Fabrication and electrochemical characterization

The electrochemical properties of the prepared powders were performed in cell matrix. For preparation of the cathode, the  $\text{LiMn}_2\text{O}_4$  or  $\text{LiCo}_{0.16}\text{Mn}_{1.84}\text{O}_4$  powders were well mixed with 5% polyvinylidene fluoride and 10% acetylene black in N-methylpyrrolidene to form a slurry. Then the slurry was brush-coated on an aluminum foil substrate, which was used as the current collector and dried in a vacuum oven maintained at  $120^\circ\text{C}$  for 4 h. The test cell was made of a cathode and a lithium metal anode

separated by a porous polypropylene film (Celgard 2400). The electrolyte used was a mixture of 1 M  $\text{LiPF}_6$ -ethylene carbonate (EC)/dimethyl carbonate (DMC) (1:1 by volume). All the assembling of the cell matrix was carried out in an argon-filled glove box. The charge/discharge cycle was performed on a battery test instrument (CT2001A, KINGNUO, China). The cell was charged and discharged between 3.4–4.35 V at C/3 at room temperature.

## 3. Result and discussion

### 3.1. Thermal analysis

The TGA and DTA results of the two mixed precursors were displayed in Figs 1 and 2. As seen in these two figures, the weight loss of the mixed precursors terminated at about  $450^\circ\text{C}$ . The weight loss between the temperature of  $110^\circ\text{C}$  and  $160^\circ\text{C}$  is due to the crystal water in the  $\text{LiMn}_2\text{O}_4$  mixed precursors. But the weight loss of temperature of the crystal water in the  $\text{LiCo}_{0.16}\text{Mn}_{1.84}\text{O}_4$  mixed precursors is between  $130^\circ\text{C}$  and  $190^\circ\text{C}$ , which is higher than that of  $\text{LiMn}_2\text{O}_4$  mixed precursors. The weight loss in the temperature range of  $270$ – $450^\circ\text{C}$  is associated with the decomposition, combustion of the constituents in the two mixed precursors and the transformation of decomposed manganese oxide and cobalt oxide, which corresponds to an exothermic peak in the curve of DTA. The exothermic peak of the  $\text{LiCo}_{0.16}\text{Mn}_{1.84}\text{O}_4$  mixed precursor is higher

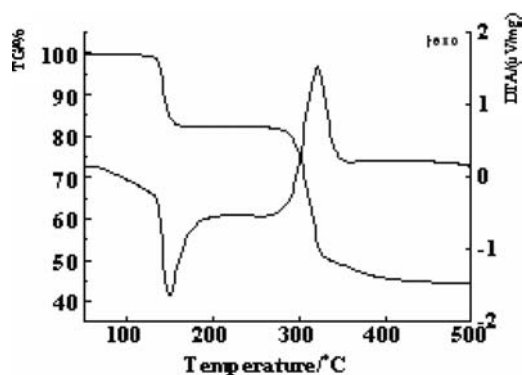


Figure 1 TGA and DTA analyses conducted on  $\text{LiMn}_2\text{O}_4$  precursor powders obtained by drying the precursor at  $90^\circ\text{C}$  for 4 h.

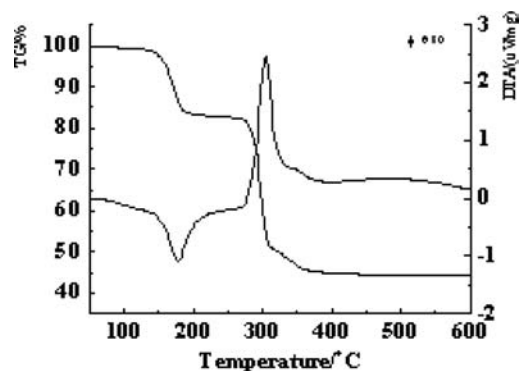


Figure 2 TGA and DTA analyses conducted on  $\text{LiCo}_{0.16}\text{Mn}_{1.84}\text{O}_4$  precursor powders obtained by drying the precursor at  $90^\circ\text{C}$  for 4 h.

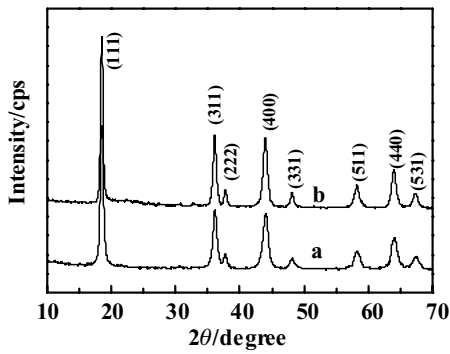


Figure 3 XRD patterns of  $\text{LiMn}_2\text{O}_4$  powders annealed at different temperature for 6 h: (a)  $450^\circ\text{C}$ ; (b)  $550^\circ\text{C}$ .

than that of the  $\text{LiMn}_2\text{O}_4$  mixed precursor, which means the heat of decomposition of the  $\text{LiCo}_{0.16}\text{Mn}_{1.84}\text{O}_4$  mixed precursor is more than that of the  $\text{LiMn}_2\text{O}_4$  mixed precursors. The reason of these phenomena may be related to the fact that Co–O bonding is stronger than that of Mn–O.

### 3.2. Crystal structure analysis

The x-ray diffraction (XRD) patterns of the  $\text{LiMn}_2\text{O}_4$  powders annealed at different temperature ( $450^\circ\text{C}$  and  $550^\circ\text{C}$ ) are shown in Fig. 3. It can be seen from the figure that the changes of diffraction peaks of the powders are not obvious as the annealing temperature increases from  $450^\circ\text{C}$  to  $550^\circ\text{C}$ , both samples have the same spinel structure. The peaks of the powders are relatively sharp and intense, which indicates that the powders are well crystallized. The higher the annealing temperature, the more complete the crystal structure. Fig. 4 shows the XRD patterns of the  $\text{LiCo}_{0.16}\text{Mn}_{1.84}\text{O}_4$  powders annealed at different temperatures ( $450^\circ\text{C}$  and  $550^\circ\text{C}$ ). It can be seen from these patterns that the variations of the peaks are similar to those of Fig. 3. In this figure there is no any characteristic diffraction peak of Co, which shows that Co exists besides the characteristic diffraction peaks of  $\text{LiMn}_2\text{O}_4$ . But the characteristic diffraction peaks of  $\text{LiMn}_2\text{O}_4$  in Fig. 4 are much more intense and smoother than that in Fig. 3, which may means that the role of Co is to substitute Mn

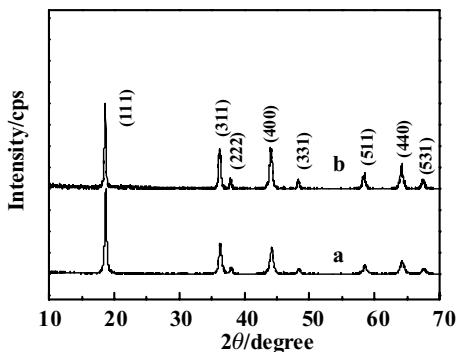


Figure 4 XRD patterns of  $\text{LiCo}_{0.16}\text{Mn}_{1.84}\text{O}_4$  powders annealed at different temperature for 6 h: (a)  $450^\circ\text{C}$ ; (b)  $550^\circ\text{C}$ .

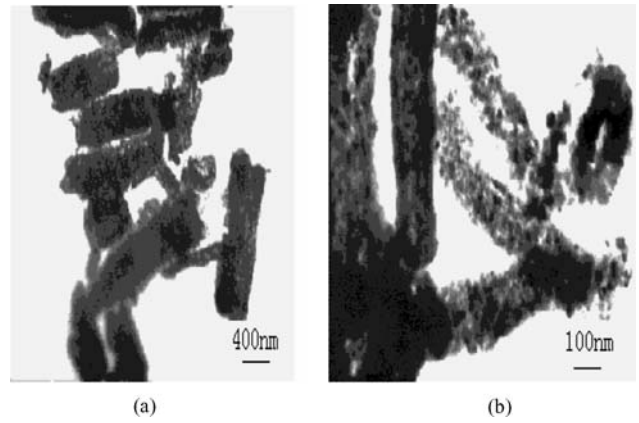


Figure 5 TEM micrographs of  $\text{LiMn}_2\text{O}_4$  powders at different annealed temperature: (a)  $450^\circ\text{C}$ ; (b)  $550^\circ\text{C}$ .

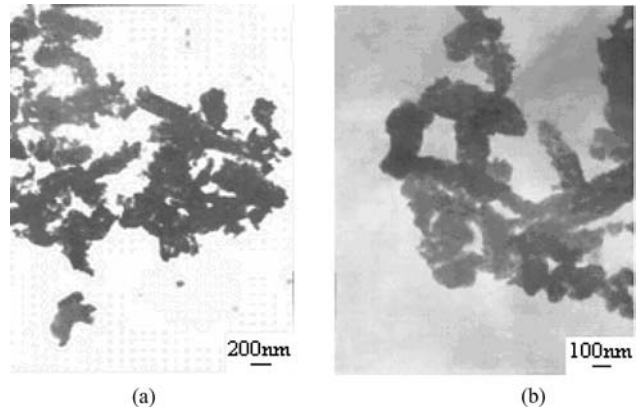


Figure 6 TEM micrographs of  $\text{LiCo}_{0.16}\text{Mn}_{1.84}\text{O}_4$  powders at different annealed temperature: (a)  $450^\circ\text{C}$ ; (b)  $550^\circ\text{C}$ .

in the spinel  $\text{LiMn}_2\text{O}_4$  skeleton to make the spinel more complete and stable. All the results show that the powders obtained are spinel structures.

### 3.3. Morphology of the particles

The transmission electron micrographs of  $\text{LiMn}_2\text{O}_4$  powders are displayed in Fig. 5. As seen from these micrographs, the grains of these powders are all round, and their diameters change from 10 to tens nanometers. But many round grains constitute solid rod-like structure. The length of the rods, as shown in Fig. 5, can be up to several micrometers and their diameters are around 200 nm. The grain become more dispersed as the annealing temperature increases from  $450^\circ\text{C}$  to  $550^\circ\text{C}$ . Fig. 6 is the transmission electron micrographs of  $\text{LiCo}_{0.16}\text{Mn}_{1.84}\text{O}_4$  powders. As shown in Fig. 6, the variation of the grains of the powders is different from that of Fig. 5, the sizes of the particles is bigger and more dispersed than that of Fig. 5 and the grains of these powders are all irregular round and are apt to reunite to agglomerate. The grain becomes also more dispersed as the annealing temperature increases from  $450^\circ\text{C}$  to  $550^\circ\text{C}$ . All the powders in both Figs 5 and 6 are nanostructure.

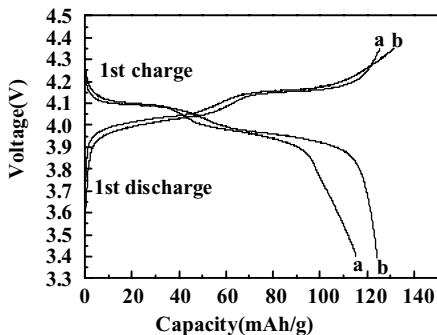


Figure 7 First charge/discharge curves of  $\text{LiMn}_2\text{O}_4$  powders annealed at different temperature for 6 h: (a)  $450^\circ\text{C}$ ; (b)  $550^\circ\text{C}$ .

### 3.4. Electrochemical properties

The first charge/discharge specific capacity of  $\text{LiMn}_2\text{O}_4$  powders annealed at different temperature are shown in Fig. 7. The figure shows that the charge specific capacity increases from 125.4 to 131.3 mAh/g and the discharge specific capacity increases from 115.3 to 124.4 mAh/g as the temperature increases from  $450^\circ\text{C}$  to  $550^\circ\text{C}$ . Fig. 8 is the first charge/discharge specific capacity of  $\text{LiCo}_{0.16}\text{Mn}_{1.84}\text{O}_4$  powders annealed at different temperature. As shown in Fig. 8, the variation of the first charge/discharge specific capacity of  $\text{LiCo}_{0.16}\text{Mn}_{1.84}\text{O}_4$  powders is similar to that of Fig. 7, and the temperature of  $550^\circ\text{C}$  may be a more suitable annealing temperature for these powders. The initial discharge capacity of the batteries decreased by substituting a part of manganese with cobalt. The initial discharge capacity of Li/LiMn<sub>2</sub>O<sub>4</sub> cell obtained in this work (annealing at  $550^\circ\text{C}$ ) was 124.4 mAh/g (theoretical capacity of  $\text{LiMn}_2\text{O}_4$  is 148 mAh/g). By substituting with Co, the initial discharge capacity (annealing at  $550^\circ\text{C}$ ) decreased to 115.2 mAh/g. This is due to the decrease of  $\text{Mn}^{3+}$  amount in substituted  $\text{LiMn}_2\text{O}_4$  since only the amount of the  $\text{Mn}^{3+}$  contributes to the charge/discharge capacity. It can be obviously seen that the discharge curves of  $\text{LiMn}_2\text{O}_4$  powders had two voltage plateaus at approximately 4.05 V and 4.10 V, which is a remarkable characteristic of a well-defined  $\text{LiMn}_2\text{O}_4$  spinel. While the discharge curves of  $\text{LiCo}_{0.16}\text{Mn}_{1.84}\text{O}_4$  powders had two

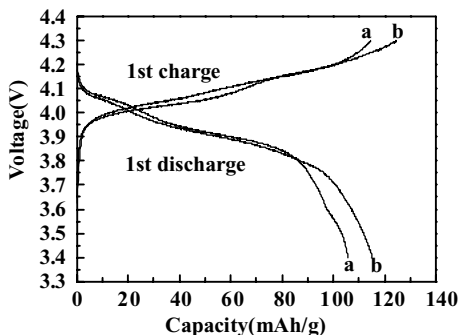


Figure 8 First charge/discharge curves of  $\text{LiCo}_{0.16}\text{Mn}_{1.84}\text{O}_4$  powders annealed at different temperature for 6 h: (a)  $450^\circ\text{C}$ ; (b)  $550^\circ\text{C}$ .

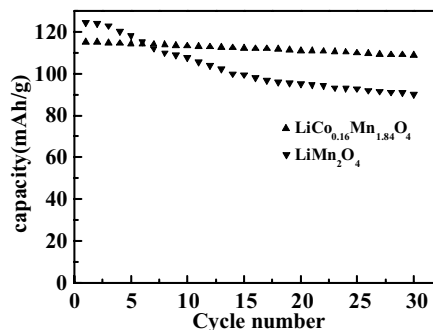


Figure 9 Cycle performance of  $\text{LiMn}_2\text{O}_4$  and  $\text{LiCo}_{0.16}\text{Mn}_{1.84}\text{O}_4$  as cathode materials for Li-ion batteries.

voltage plateaus ranging at approximately 4.05–4.08 V and 3.90–3.95 V, and the two voltage plateaus are not as clear as that of  $\text{LiMn}_2\text{O}_4$ . From charge/discharge curves, it is found that lithium ion was reversibly lithiated/delithiated through  $\text{LiMn}_2\text{O}_4$  spinel framework. Fig. 9 shows the cycle performance of the  $\text{LiMn}_2\text{O}_4$  and  $\text{LiCo}_{0.16}\text{Mn}_{1.84}\text{O}_4$  annealing at  $550^\circ\text{C}$  as cathode materials for Li-ion batteries, respectively. Comparing with the poor cycle performance occurred with  $\text{LiMn}_2\text{O}_4$  cathode, the substituted spinel exhibited a remarkable improvement of cycle behavior. After 30 times charge/discharge cycles, the capacity loss of  $\text{LiCo}_{0.16}\text{Mn}_{1.84}\text{O}_4$  sample was only 5.5%, but the capacity loss of  $\text{LiMn}_2\text{O}_4$  sample increased up to 28%. This suggests that the substituted spinel  $\text{LiCo}_{0.16}\text{Mn}_{1.84}\text{O}_4$  show a good cycle life.

### 4. Conclusion

$\text{LiMn}_2\text{O}_4$  and its substituted forms spinel  $\text{LiCo}_{0.16}\text{Mn}_{1.84}\text{O}_4$  have been prepared by simply annealing the mixed precursors which were synthesized by low heating solid state coordination method. All of the as-prepared powders were identified as a single spinel phase. The powders had a spherical morphology and became more and more agglomerated as the annealing temperature increased. The first discharge capacity of  $\text{LiMn}_2\text{O}_4$  annealed at  $550^\circ\text{C}$  was up to 124.4 mAh/g though its cycle performance was poor. The substituted spinel  $\text{LiCo}_{0.16}\text{Mn}_{1.84}\text{O}_4$  showed better cycle life than that of  $\text{LiMn}_2\text{O}_4$ , the discharge capacity loss of  $\text{LiCo}_{0.16}\text{Mn}_{1.84}\text{O}_4$  was only 5.5% after 30 cycles. Thus, it can be seen that low heating solid state coordination method is an effective method to prepare lithium manganese oxide  $\text{LiMn}_2\text{O}_4$  and its substituted forms.

### Acknowledgements

This work has been partially supported by the National Nature Science Foundation of China (Grant No.20161003) and the Starting Foundation for Younger Teacher's Scientific Research of Xinjiang University (Grant No.QN040106)

## References

1. J. M. TARASCON, E. WANG, F. K. SHOKOOHI, W. R. MCKINNON and S. COLSON, *J. Electrochem. Soc.* **138** (1991) 2859.
2. T. OHZUKU, M. KITAGAWA and T. HIRAI, *J. Electrochem. Soc.* **137** (1990) 769.
3. J. M. TARASCON and D. GUYOMARD, *Electrochim. Acta* **38** (1993) 1221.
4. G. PISTOIA, G. WANG and C. WANG, *Solid State Ionics* **58** (1992) 285.
5. H. HUANG and P. G. BRUCE, *J. Power Sources* **54** (1995) 52.
6. J. M. TARASCON, W. R. MCKINNON, F. COOWAR, T. N. BOWMER, G. AMATUCCI and D. GUYOMARD, *J. Electrochem. Soc.* **141** (1994) 1421.
7. R. J. GOMMOW, A. DE KOCK and M. M. THACKERAY, *Solid State Ionics* **69** (1994) 59.
8. Y. XIA, H. NOGUCHI and M. YOSHIO, *J. Solid State Chem.* **119** (1995) 216.
9. R. BITTIHN, R. HERR and D. HOGE, *J. Power Sources* **43** 44 (1993) 223.
10. L. GUOHUA, H. IKUTA, T. UCHIDA and M. WAKIHARA, *J. Electrochem. Soc.* **143** (1996) 178.
11. D. SONG, H. IKUTA, T. UCHIDA and M. WAKIHARA, *Solid State Ionics* **117** (1999) 151.
12. M. WAKIHARA, G. LI, H. IKUTA, in *Lithium Ion Batteries*, M. WAKIHARA, O. YAMAMOTO (eds.), (Kodansha, Tokyo 1998) p. 26.
13. X. QIU, X. SUN, W. SHEN, N. CHEN, *Solid State Ionics* **93** (1997) 335.
14. H. HUANG and P. G. BRUCE, *J. Electrochem. Soc.* **141** (1994) L106.
15. X. Q. XIN and L. M. ZHENG, *ibid.* **106** (1993) 451.
16. J. P. LANG, X. Q. XIN, *J. Solid State Chem.* **108** (1994) 118.
17. X. B. YAO, L. M. ZHENG and X. Q. XIN, *J. Solid State Chem.* **117** (1995) 333.
18. D. Z. JIA, J. Q. YU and X. XIA, *Chinese Sci. Bull.* **43** (1998) 571.
19. X. R. YE, D. Z. JIA, J. Q. YU, X. Q. XIN and Z. L. XUE, *Adv. Mater.* **11** (1999) 941.

*Received 9 June  
and accepted 24 August 2005*